Electronic Supplementary Material (ESI) for Nanoscale.

Supporting Information For

Near-Infrared Emitting Dual-Stimuli-Responsive Carbon Dots from Endogenous Bile Pigments

*Parinaz Fathi, Parikshit Moitra, Madeleine M. McDonald, Mandy B. Esch, Dipanjan Pan**

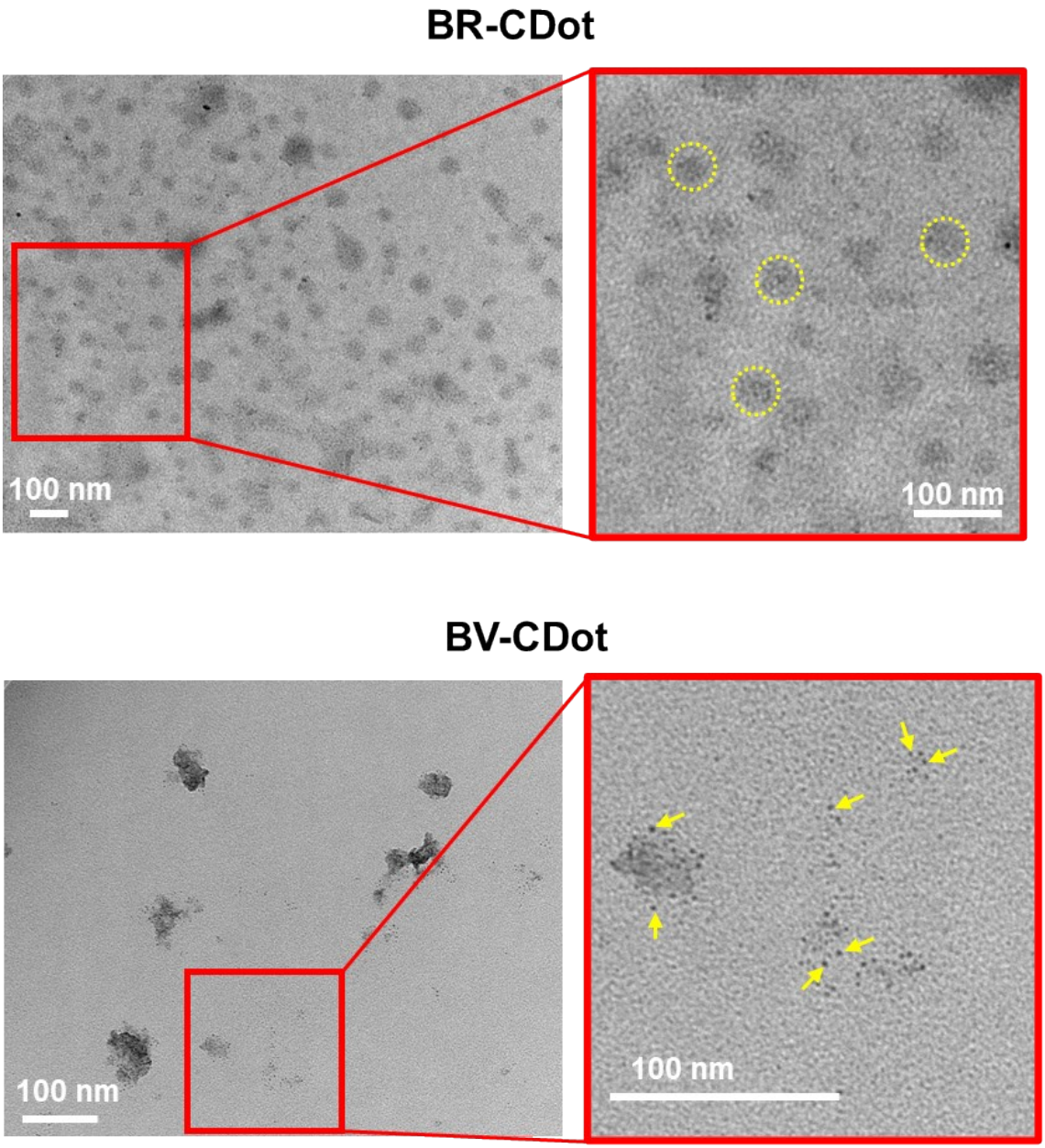

Figure S1. TEM images of BR-CDots and BV-CDots confirm successful nanoparticle synthesis. Yellow arrows and dashed outlines indicate some examples of nanoparticles. BV-Cdots are smaller than BR-CDots.

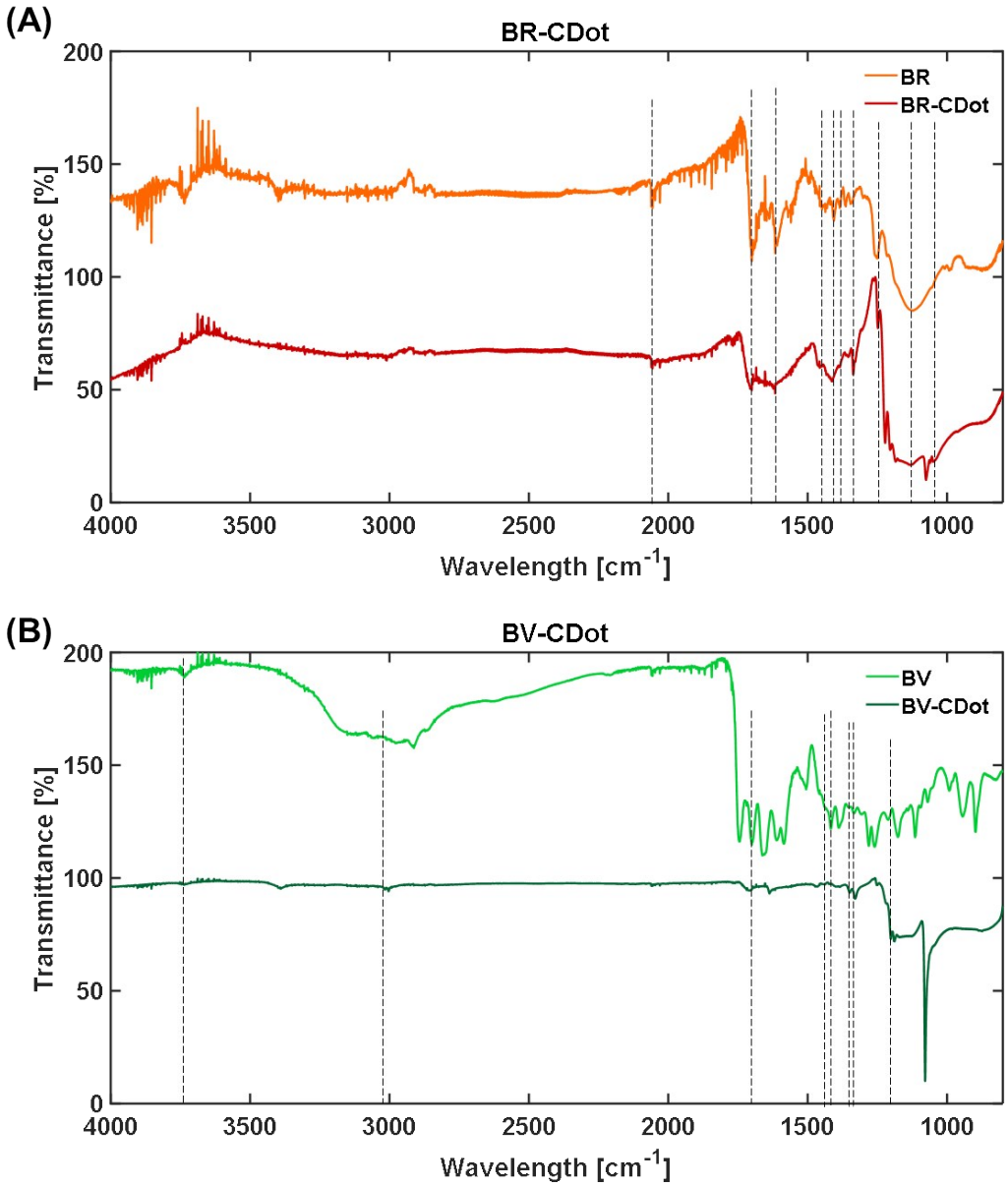

Figure S2. FT-IR Spectra of (A) Bilirubin (BR) and BR-CDot and (B) Biliverdin (BV) and BV-CDot. Dashed lines depict peaks that are seen in both the precursor and the nanoparticle. Retention of some FT-IR peaks in the carbon dots suggests that some imidolic structures from the precursors are retained by the carbon dots.

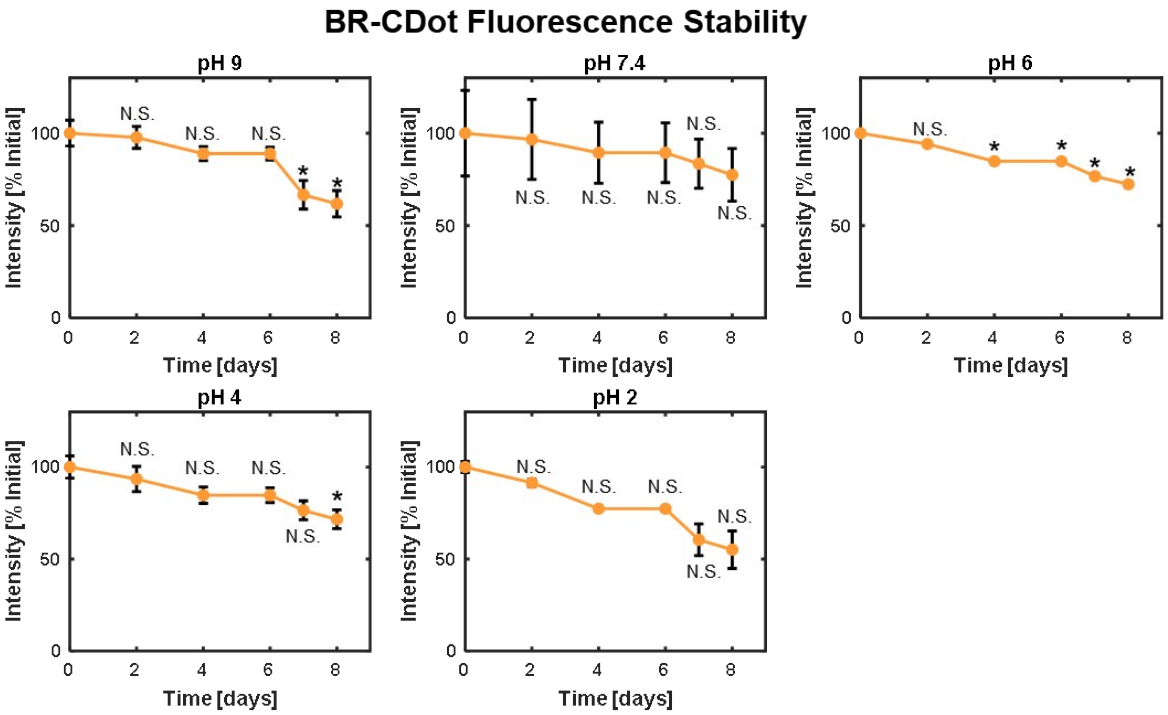

Figure S3. Fluorescence stability of BR-CDots incubated at 37 °C under different pH conditions for 8 days. Data is presented is a percentage of the initial fluorescence intensity. Each data point represents an average of two trials, and error bars represent standard deviation. N.S. indicates there is not a statistically significant difference from the initial fluorescence intensity. * indicates statistical significance ($P<0.05$) as determined by a Student's T test.

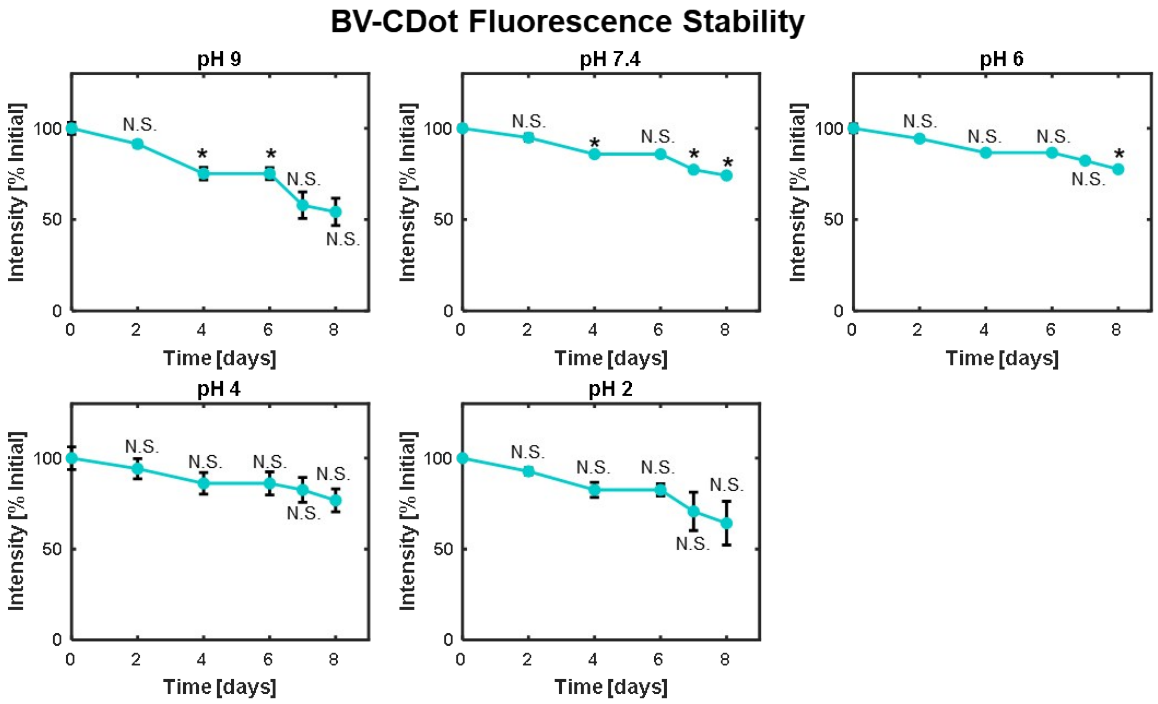

Figure S4. Fluorescence stability of BV-CDots incubated at 37 °C under different pH conditions for 8 days. Data is presented is a percentage of the initial fluorescence intensity. Each data point represents an average of two trials, and error bars represent standard deviation. N.S. indicates there is not a statistically significant difference from the initial fluorescence intensity. * indicates statistical significance ($P<0.05$) as determined by a Student's T test.

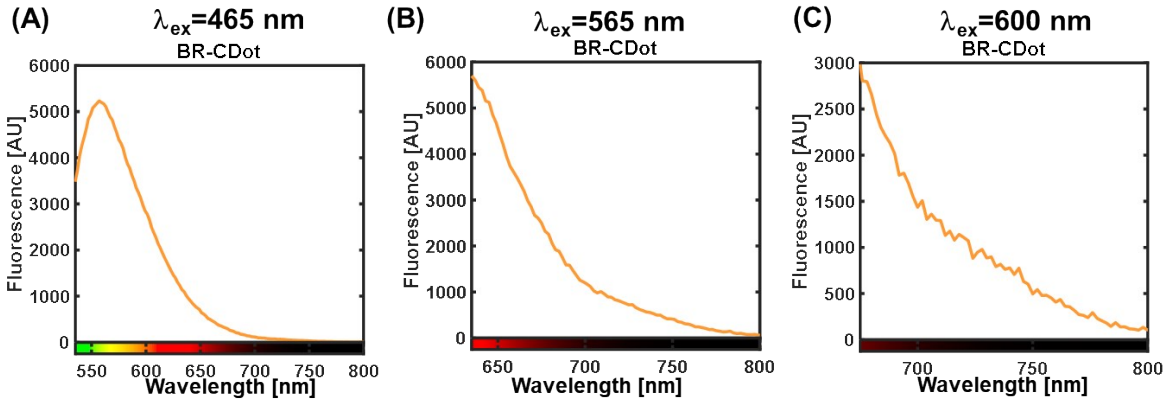

Figure S5. Fluorescence spectra of BR-CDots for excitation wavelengths of 465 nm **(A)**, 565 nm **(B)**, and 600 nm.

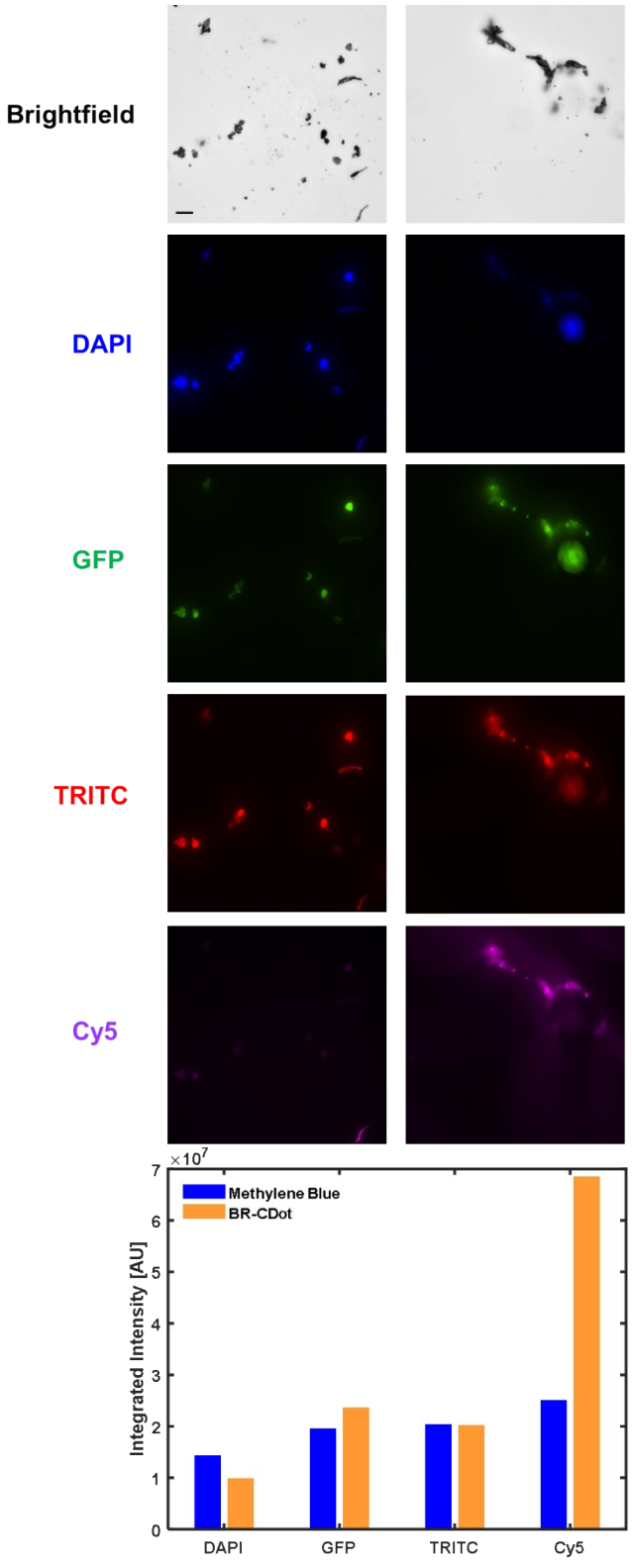

Figure S6. Fluorescence images of drop-casted solutions of methylene blue and BR-CDots using different filters. Scale bar represents 50 μm. The scale is the same for all images.

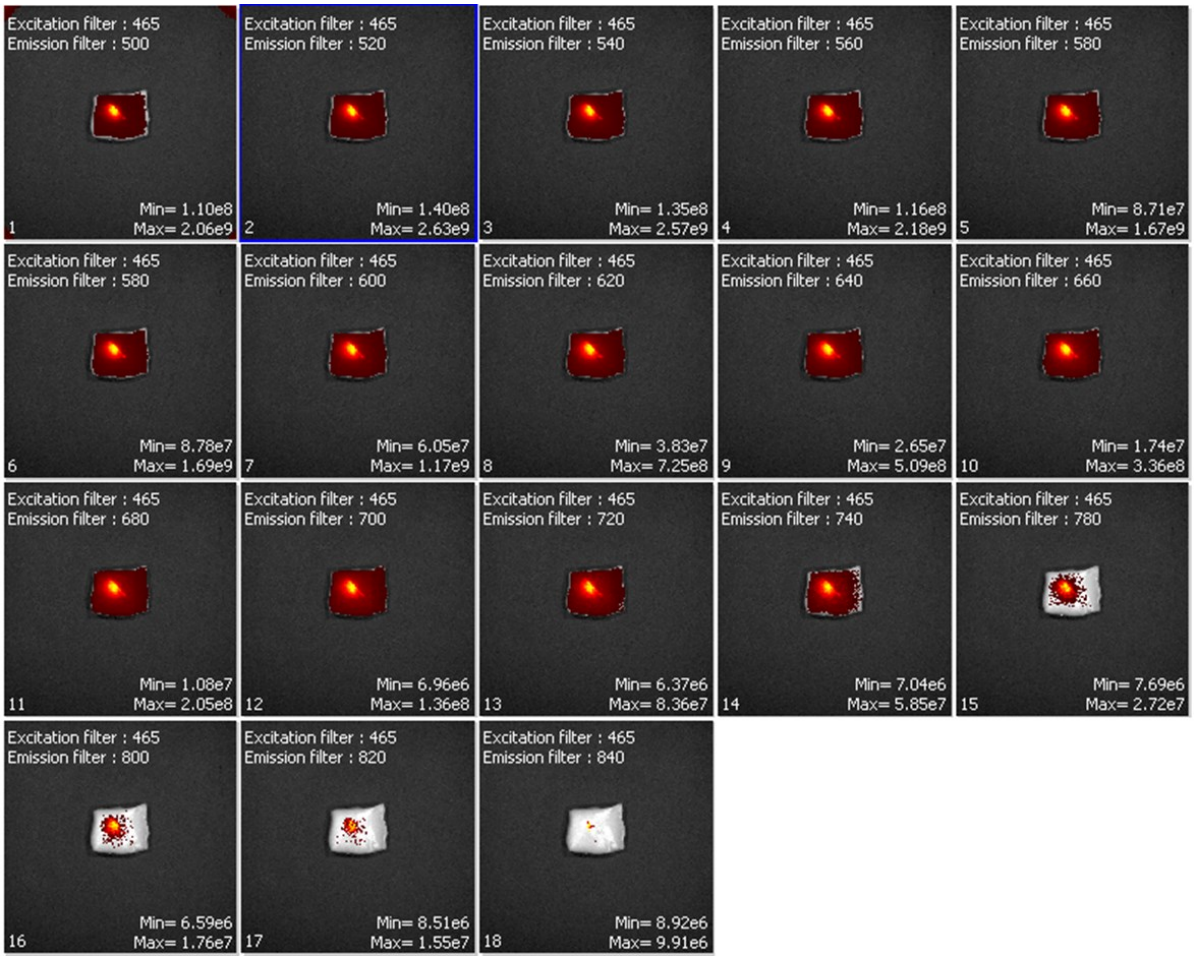

Figure S7. IVIS tissue phantom images of surface-injected BR-CDots for excitation wavelength of 465 nm and emissions in the range of 500 nm-840 nm.

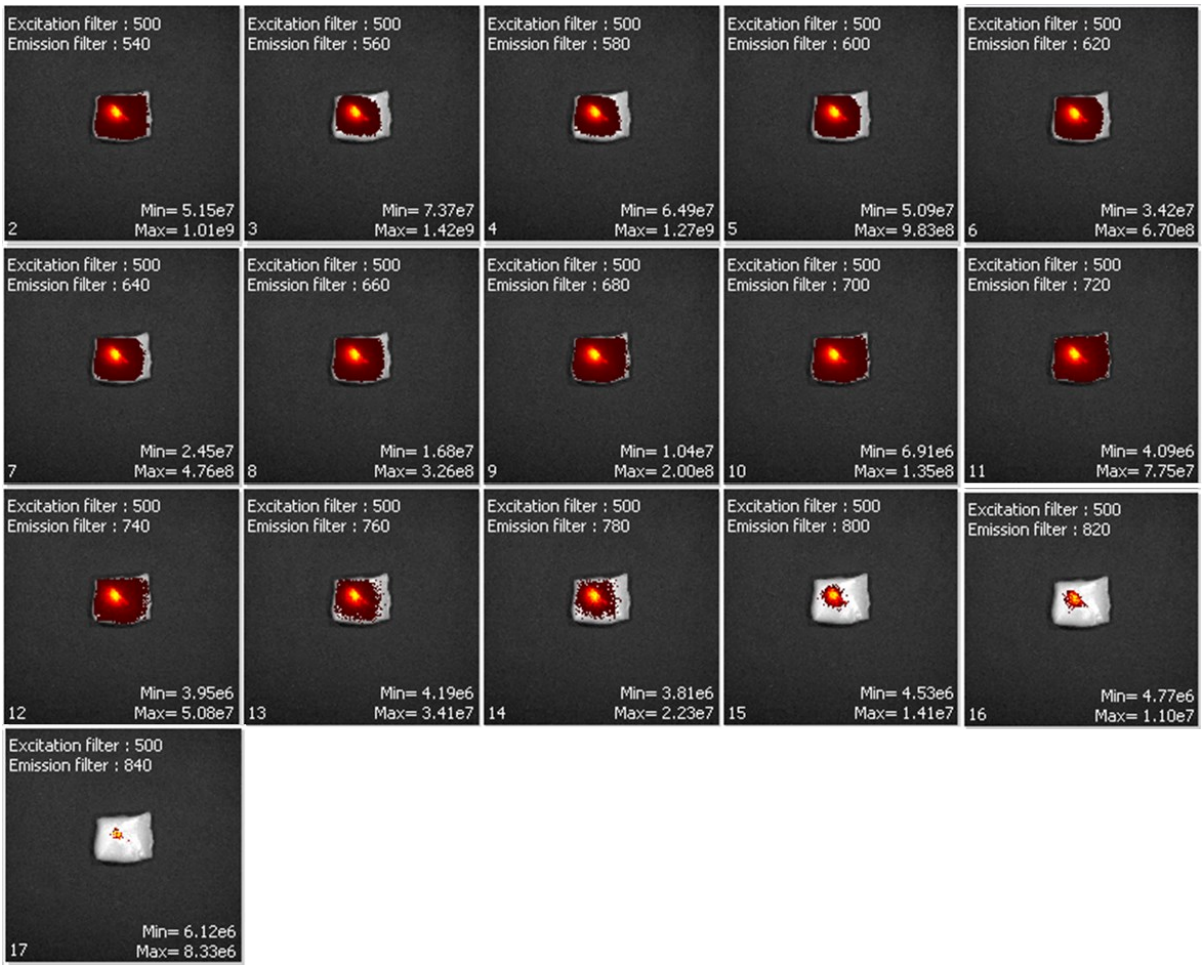

Figure S8. IVIS tissue phantom images of surface-injected BR-CDots for excitation wavelength of 500 nm and emissions in the range of 540 nm-840 nm.

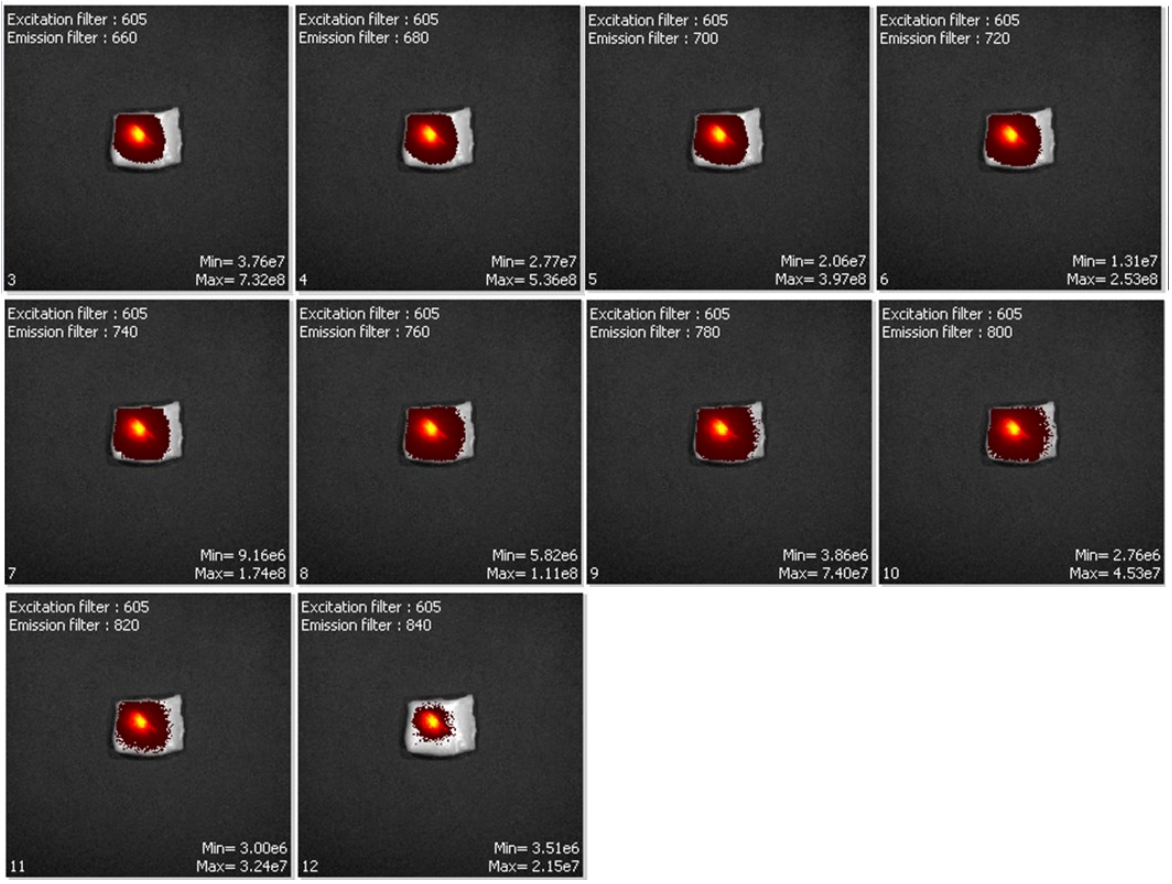

Figure S9. IVIS tissue phantom images of surface-injected BR-CDots for excitation wavelength of 605 nm and emission wavelengths in the range of 660 nm-840 nm.

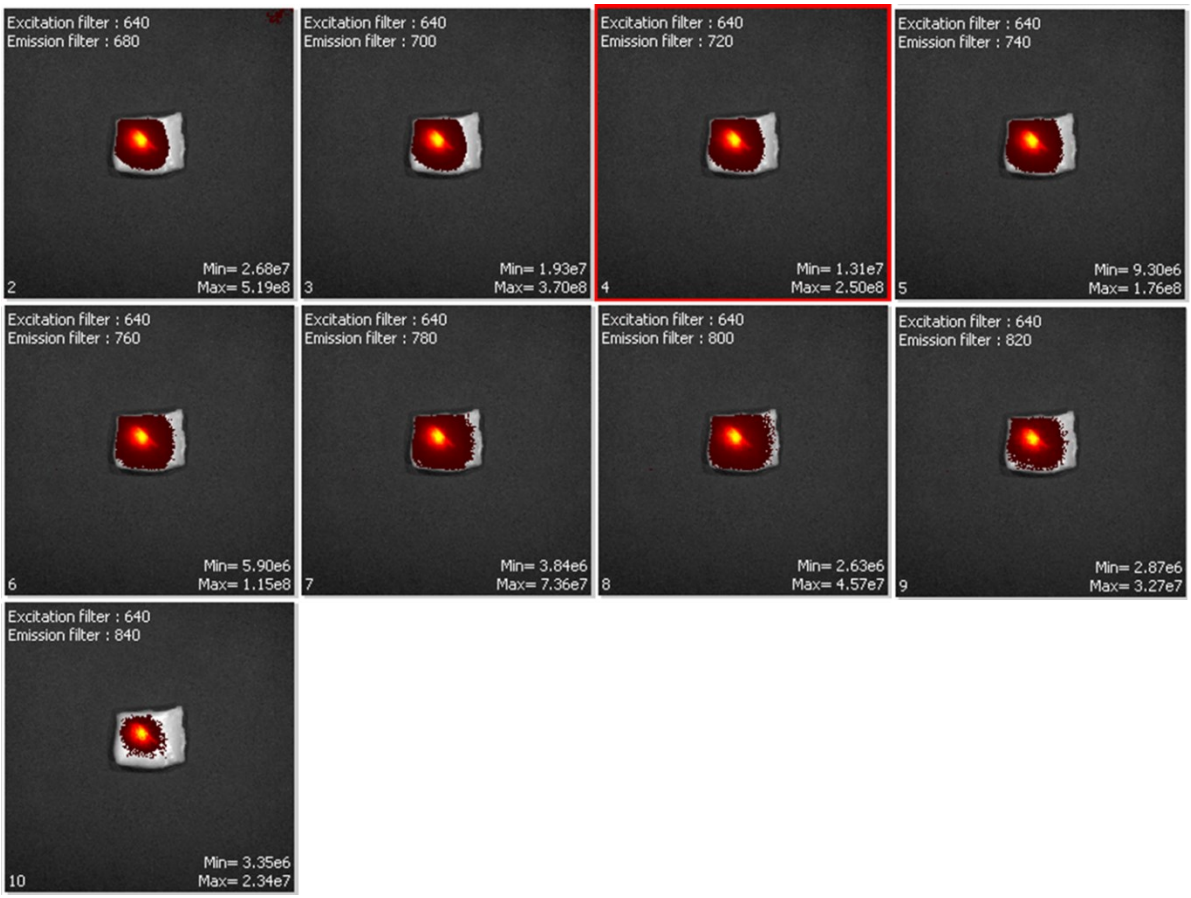

Figure S10. IVIS tissue phantom images of surface-injected BR-CDots for excitation wavelength of 640 nm and emission wavelengths in the range of 680 nm-840 nm.

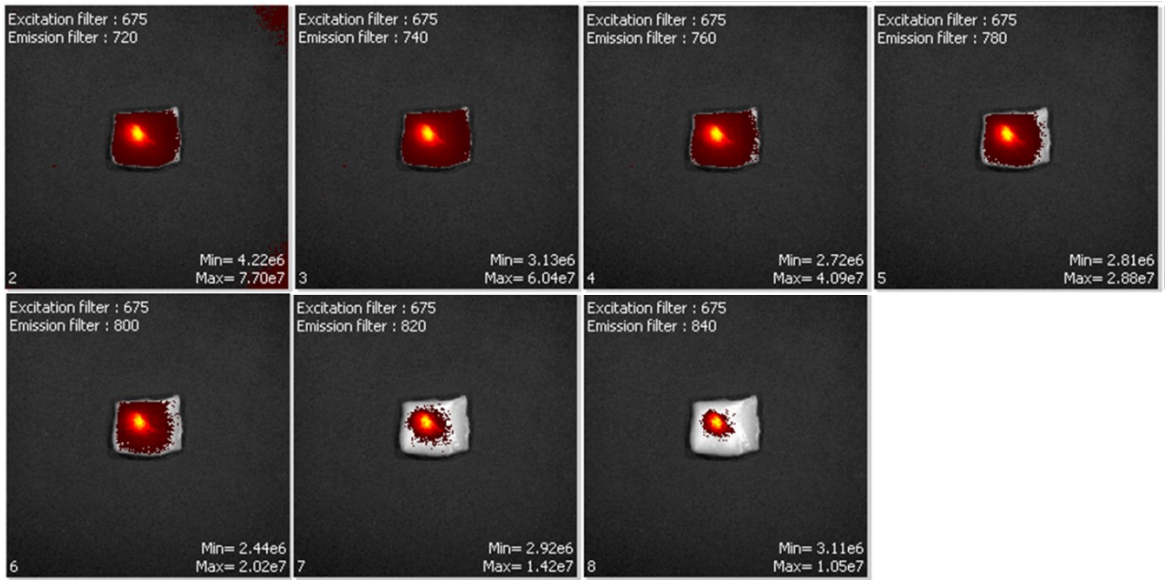

Figure S11. IVIS tissue phantom images of surface-injected BR-CDots for excitation wavelength of 675 nm and emission wavelengths in the range of 720 nm-840 nm.

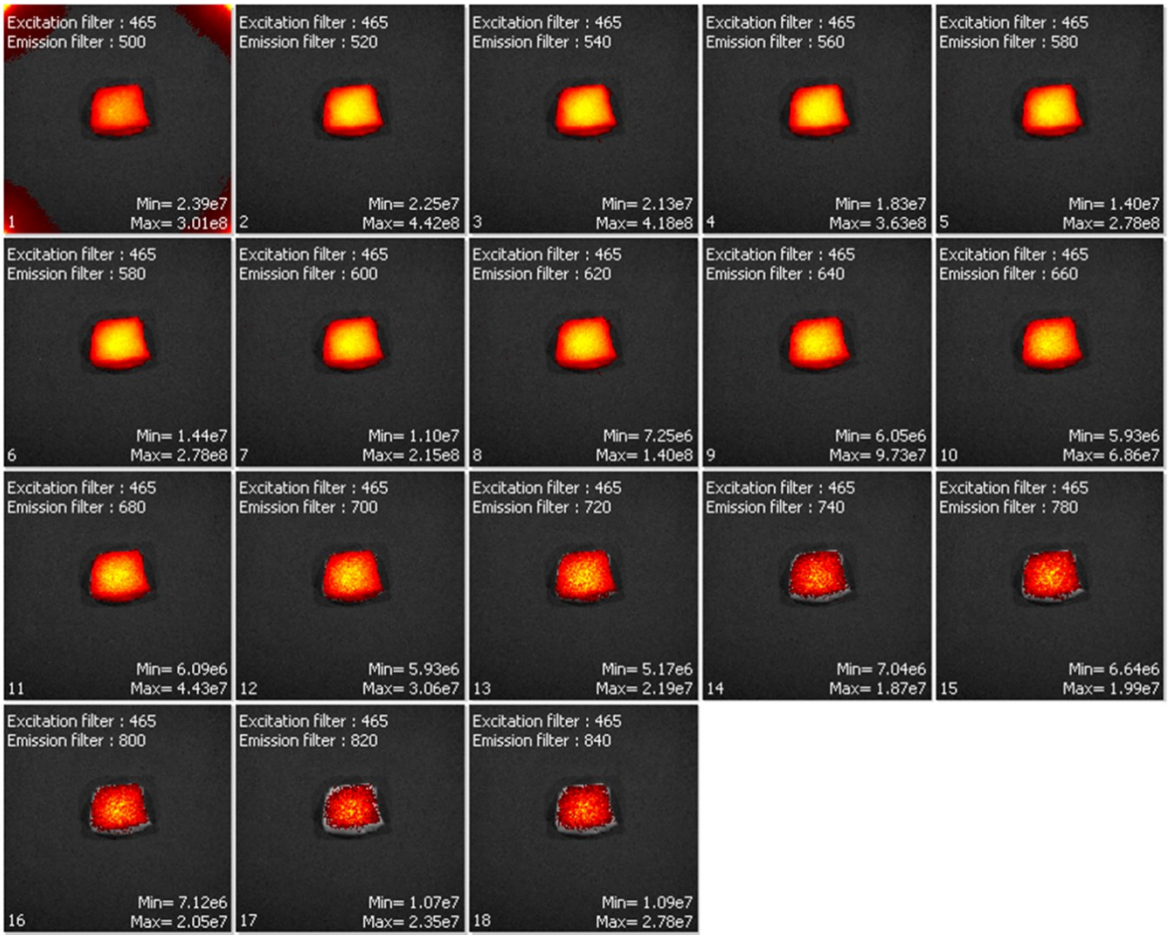

Figure S12. IVIS tissue phantom images of 8.5-mm deep BR-CDots for excitation wavelength of 465 nm and emission wavelengths in the range of 500 nm-840 nm.

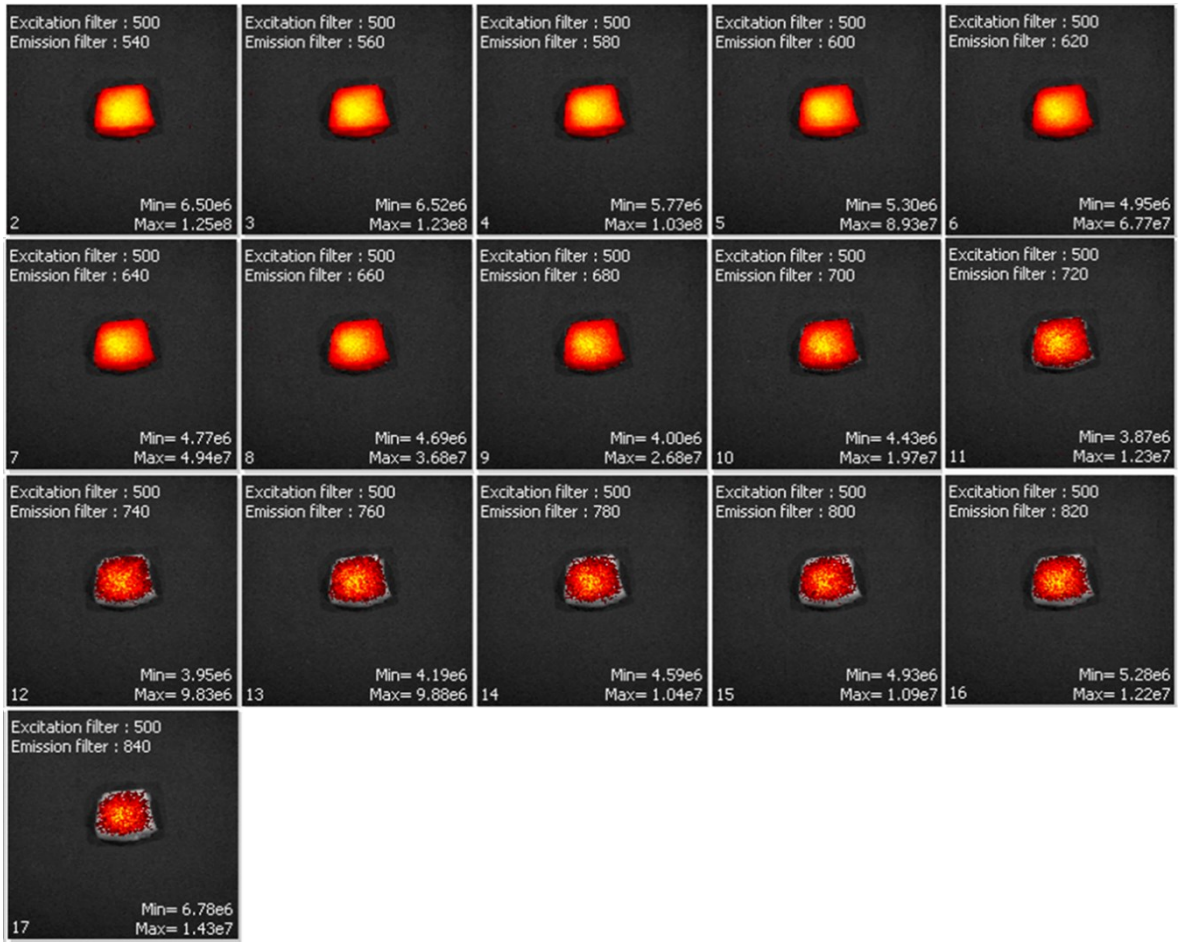

Figure S13. IVIS tissue phantom images of 8.5-mm deep BR-CDots for excitation wavelength of 500 nm and emission wavelengths in the range of 540 nm-840 nm.

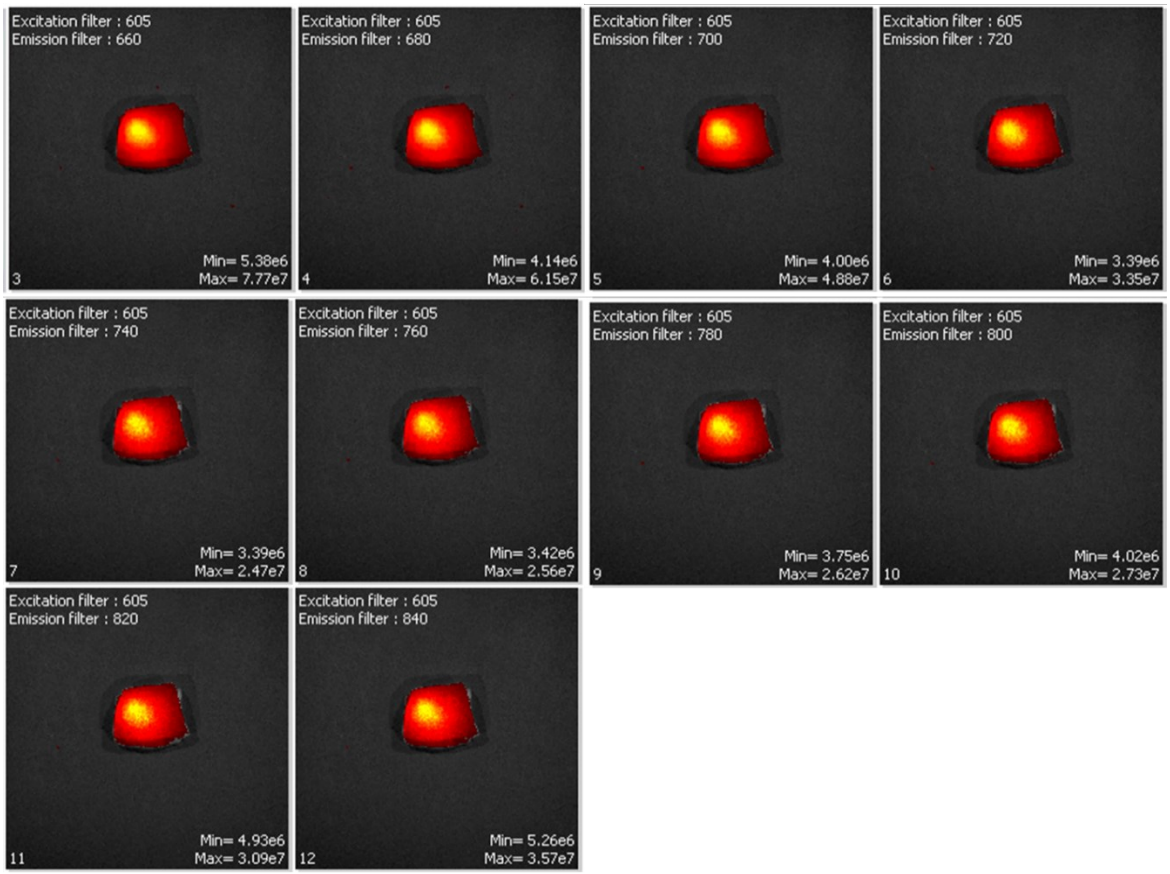

Figure S14. IVIS tissue phantom images of 8.5-mm deep BR-CDots for excitation wavelength of 605 nm and emission wavelengths in the range of 660 nm-840 nm.

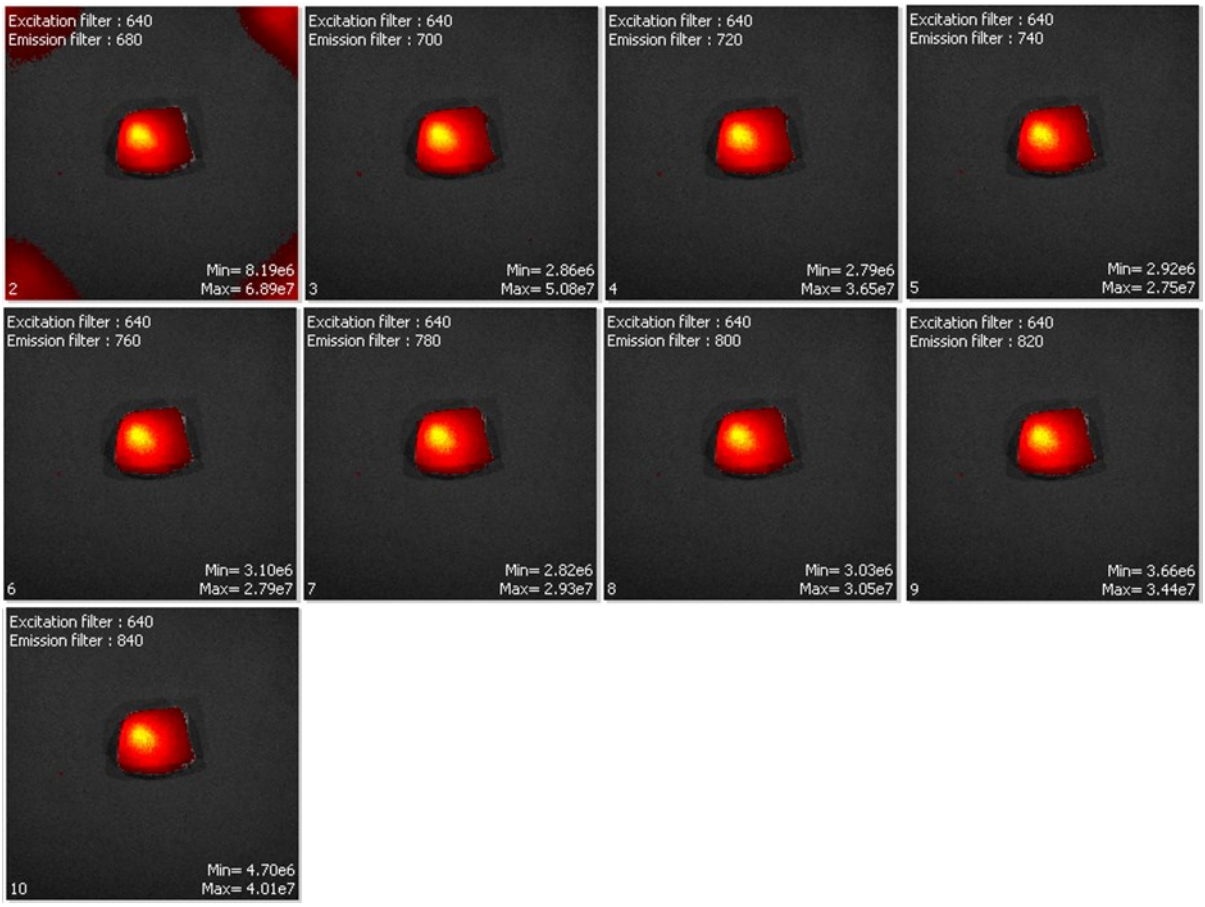

Figure S15. IVIS tissue phantom images of 8.5-mm deep BR-CDots for excitation wavelength of 640 nm and emission wavelengths in the range of 680 nm-840 nm.

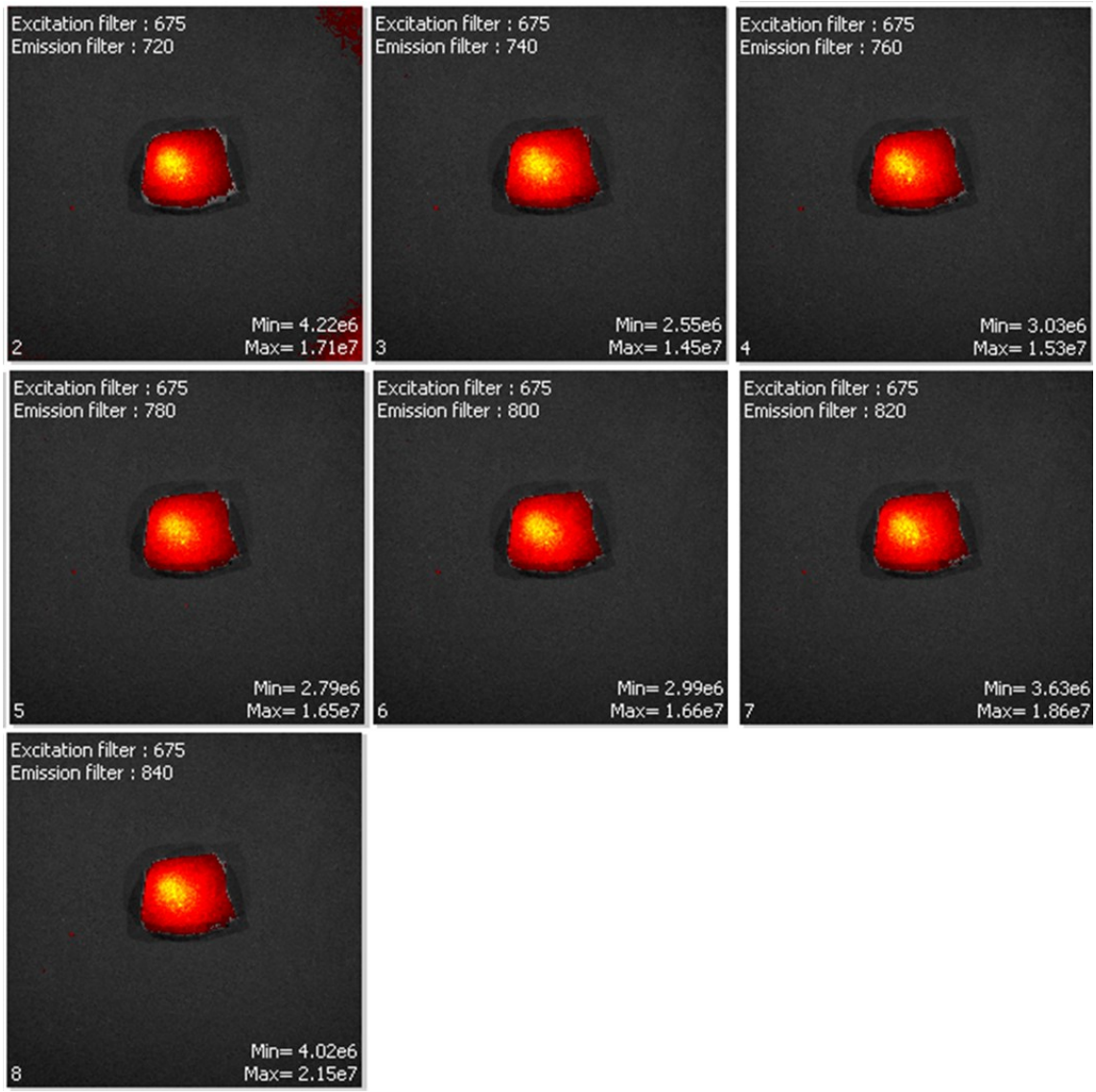

Figure S16. IVIS tissue phantom images of 8.5-mm deep BR-CDots for excitation wavelength of 675 nm and emission wavelengths in the range of 720 nm-840 nm.

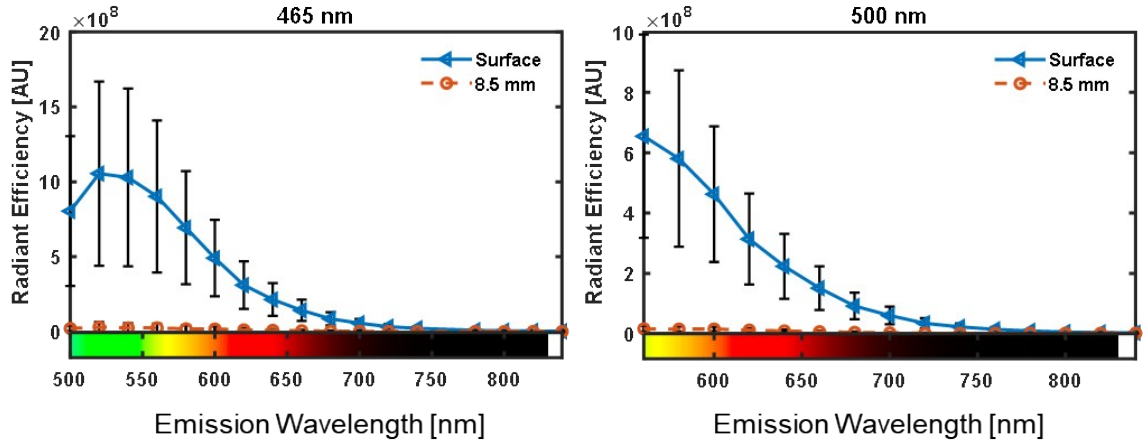

Figure S17. ROI analysis for BR-CDots in chicken tissue at excitation wavelengths of 465 nm and 500 nm.

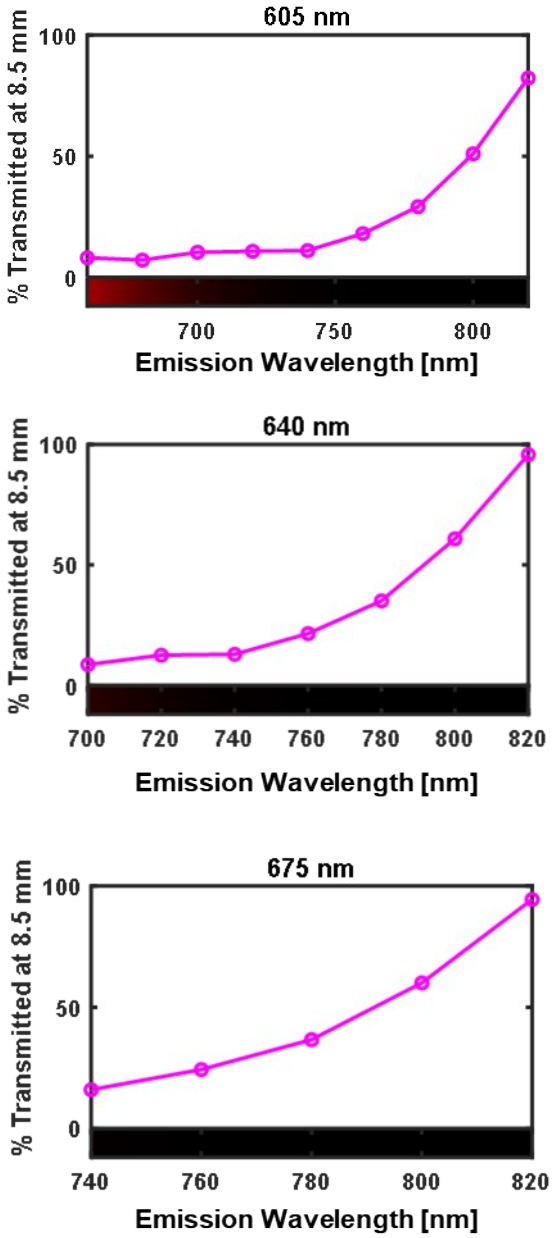

Figure S18. Percentage of signal transmitted through 8.5 mm tissue. Data is presented as a percentage ratio of the background-subtracted average radiant efficiency at 8.5 mm depth to the background-subtracted average radiant efficiency at the surface level. The percentage of nanoparticle signal transmitted increases with an increase in emission wavelength. This trend holds true across excitation wavelengths of 605 nm, 640 nm, and 675 nm.

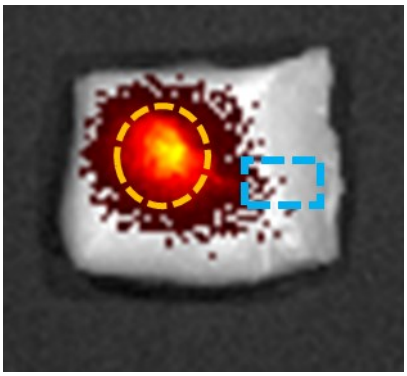

Figure S19. Example ROIs for tissue phantom image. Yellow oval outlines BR-CDot ROI and blue rectangle outlines background ROI.

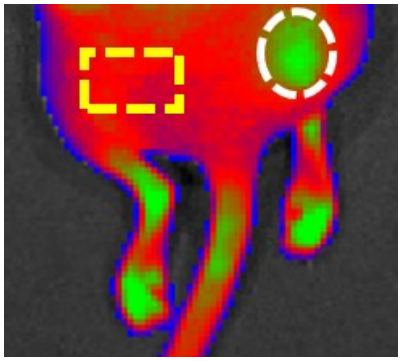

Figure S20. Example ROIs for *ex vivo* mouse imaging. White oval outlines BR-CDot ROI and yellow rectangle outlines background ROI.